2002/02/04
US-Japan Workshop on RF Physics and
Profile Control and Steady State Operation using RF
Kyushu Univ, Chikushi Campus

Analysis of ICRF and Alfvén Waves in Toroidal Plasmas

A. Fukuyama
Department of Nuclear Engineering,
Kyoto University, Kyoto 606-8501, Japan

Contents

- Full Wave Code TASK/WM
- ICRF Waves in Toroidal Helical Plasmas
- Alfvén Eigenmode driven by Energetic Ions
- Summary

Full Wave Analysis in Toroidal Devices

- **Motivations**
  - RF Heating and Current Drive (Fast wave, Alfvén wave)
  - Low Frequency Instabilities (Alfvén eigenmodes)
  - Diagnostics (Ion cyclotron emission)
- **Features**
  - Configuration: 2D (Axi-symmetric, Linear-helical), 3D
  - Plasma model: Cold, Hot (No FLR), FLR (Fast wave, Differential, Integral)
  - Numerical method: Finite difference, Finite element, Mode expansion
- **Various Codes**

  ALCYON (Cadarache), LION (Lausanne/JET), PENN (Stockholm), PICES (Oak Ridge), TASK/WM (Ours), TORIC (Garching), Bonoli (MIT)

Full Wave Code: TASK/WM

- **Magnetic Flux Coordinates** **(Non-Orthogonal)**
  - Minor radius direction: Poloidal Magnetic Flux ψ
  - Poloidal direction: θ
  - Toroidal direction: φ

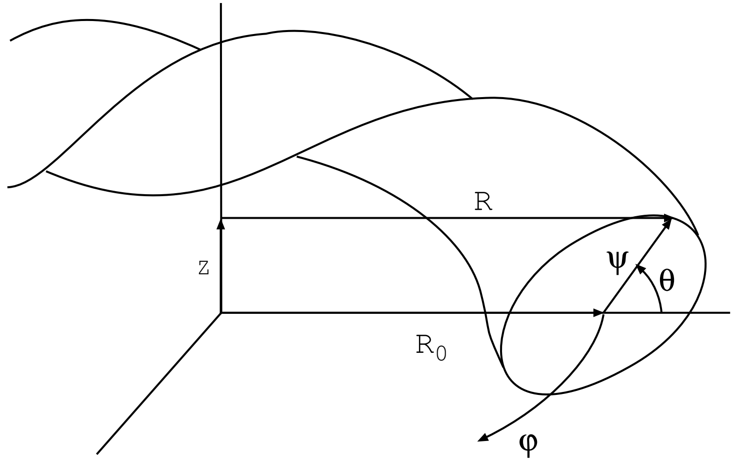

- **Co-variant expression** of $\boldsymbol{E}$

$$\boldsymbol{E} = E_1\boldsymbol{e}^1 + E_2\boldsymbol{e}^2 + E_3\boldsymbol{e}^3$$

where contra-variant basis

$$\boldsymbol{e}^1 = \nabla\psi, \qquad \boldsymbol{e}^2 = \nabla\theta, \qquad \boldsymbol{e}^3 = \nabla\varphi$$

- J **: Jacobian** $\quad J = \dfrac{1}{\boldsymbol{e}^1 \cdot \boldsymbol{e}^2 \times \boldsymbol{e}^3} = \dfrac{1}{\nabla\psi \cdot \nabla\theta \times \nabla\varphi}$
- g **: Metric tensor** $\quad g_{ij} = \boldsymbol{e}_i \cdot \boldsymbol{e}_j$, where co-variant basis $\boldsymbol{e}_i \equiv \partial\boldsymbol{r}/\partial x_i$

Wave Equation

- **Maxwell's equation** for stationary wave electric field $\boldsymbol{E}$
  (angular frequency ω, light velocity cj

$$\nabla \times \nabla \times \boldsymbol{E} = \frac{\omega^2}{c^2} \overleftrightarrow{\epsilon} \cdot \boldsymbol{E} + \mathrm{i}\,\omega \mu_0 \boldsymbol{j}_{\mathrm{ext}}$$

  - $\overleftrightarrow{\epsilon}$ **: Dielectric Tensor** : Effects of finite temperature
    Cyclotron damping, Landau damping
  - $\boldsymbol{j}_{\mathrm{ext}}$: Antenna Current

- **Wave Equation in Non-Orthogonal Coordinates** (radial components)

$$(\nabla \times \nabla \times \boldsymbol{E})^1 = \frac{1}{J}\left[\frac{\partial}{\partial x^2}\left\{\frac{g_{31}}{J}\left(\frac{\partial E_3}{\partial x^2} - \frac{\partial E_2}{\partial x^3}\right) + \frac{g_{32}}{J}\left(\frac{\partial E_1}{\partial x^3} - \frac{\partial E_3}{\partial x^1}\right) + \frac{g_{33}}{J}\left(\frac{\partial E_2}{\partial x^1} - \frac{\partial E_1}{\partial x^2}\right)\right\}\right.$$
$$\left. - \frac{\partial}{\partial x^3}\left\{\frac{g_{21}}{J}\left(\frac{\partial E_3}{\partial x^2} - \frac{\partial E_2}{\partial x^3}\right) + \frac{g_{22}}{J}\left(\frac{\partial E_1}{\partial x^3} - \frac{\partial E_3}{\partial x^1}\right) + \frac{g_{23}}{J}\left(\frac{\partial E_2}{\partial x^1} - \frac{\partial E_1}{\partial x^2}\right)\right\}\right]$$

  - $(x^1, x^2, x^3) = (\psi, \theta, \varphi)$
  - Similar expression for poloidal and toroidal components

Response of Plasmas

- Usually the dielectric tensor $\overleftrightarrow{\epsilon}$ is calculated in Cartesian coordinates with static magnetic field along the z axis.
- **Local normalized orthogonal coordinates**

$$\hat{\boldsymbol{e}}_s = \frac{\boldsymbol{\nabla}\psi}{|\boldsymbol{\nabla}\psi|}, \quad \hat{\boldsymbol{e}}_b = \hat{\boldsymbol{e}}_h \times \hat{\boldsymbol{e}}_\psi, \quad \hat{\boldsymbol{e}}_h = \frac{\boldsymbol{B}_0}{|\boldsymbol{B}_0|}$$

- Variable Transformation: $\overleftrightarrow{\mu}$

$$\begin{pmatrix} E_1 \\ E_2 \\ E_3 \end{pmatrix} = \overleftrightarrow{\mu} \cdot \begin{pmatrix} E_s \\ E_b \\ E_h \end{pmatrix}$$

$$\overleftrightarrow{\mu} \equiv \begin{pmatrix} \dfrac{1}{\sqrt{g^{11}}} & \dfrac{d}{\sqrt{Jg^{11}}} & c_2 g_{12} + c_3 g_{13} \\ 0 & c_3 J\sqrt{g^{11}} & c_2 g_{22} + c_3 g_{23} \\ 0 & -c_2 J\sqrt{g^{11}} & c_2 g_{32} + c_3 g_{33} \end{pmatrix}$$

$$c_2 = B^\theta/B, \quad c_2 = B^\phi/B$$
$$d = c_2(g_{23}g_{12} - g_{22}g_{31}) + c_3(g_{33}g_{12} - g_{32}g_{31})$$
$$g^{11} = (g_{22}g_{33} - g_{23}g_{32})/J^2$$

- **Dielectric Tensor in Non-Orthogonal Coordinates**:

$$\boxed{\overleftrightarrow{\epsilon} = \overleftrightarrow{\mu} \cdot \overleftrightarrow{\epsilon}_{sbh} \cdot \overleftrightarrow{\mu}^{-1}}$$

Fourier Mode Expansion

- **Fourier Expansion in Poloidal and Toroidal Directions**
- Spatial variation of wave electric field, medium and the L.H.S. of Maxwell's equation

$$E(\psi,\theta,\varphi) = \sum_{mn} E_{mn}(\psi) e^{\mathrm{i}(m\theta+n\varphi)}$$

$$G(\psi,\theta,\varphi) = \sum_{lk} G_{lk}(\psi) e^{\mathrm{i}(l\theta+kN_p\varphi)}$$

$$J(\boldsymbol{\nabla}\times\boldsymbol{\nabla}\times\boldsymbol{E}) = G(\psi,\theta,\varphi)E(\psi,\theta,\varphi) = \sum_{m'n'} [J(\boldsymbol{\nabla}\times\boldsymbol{\nabla}\times\boldsymbol{E})]_{m'n'} e^{\mathrm{i}(m'\theta+n'\varphi)}$$

- **Coupling between various modes** (N_h : Rotation number of helical coil in φ)

Mode Number	Toroidal Direcition	Poloidal Direction
Wave electric field $\boldsymbol{E}$	n	m
Medium G	kN_h	l
$J(\boldsymbol{\nabla}\times\boldsymbol{\nabla}\times\boldsymbol{E})$	n'	m'
Relations	$n' = n + kN_\mathrm{h}$	$m' = m + l$

Parallel Wave Number

- **Dielectric tensor** $\overleftrightarrow{\epsilon}(\psi,\theta,\varphi,k_{\parallel}^{m''n''})$ depends on **parallel wave number** $k_{\parallel}^{m'',n''}$ through the **plasma dispersion function** $Z[(\omega - N\omega_{\rm cs})/k_{\parallel}^{m''n''}v_{\rm Ts}]$

$$
\begin{aligned}
k_{\parallel}^{m'',n''} &= -i\hat{\boldsymbol{e}}_h\cdot\boldsymbol{\nabla} = -i\hat{\boldsymbol{e}}_h\cdot(\boldsymbol{\nabla}\theta\frac{\partial}{\partial\theta}+\boldsymbol{\nabla}\varphi\frac{\partial}{\partial\varphi}) \\
&= -i\hat{\boldsymbol{e}}_h\cdot(\boldsymbol{e}^2\frac{\partial}{\partial\theta}+\boldsymbol{e}^3\frac{\partial}{\partial\varphi}) = m''\frac{B^\theta}{|B|}+n''\frac{B^\varphi}{|B|}
\end{aligned}
$$

- **Fourier components of electric displacement**

$$
\begin{array}{ccccccccccc}
(J\overleftrightarrow{\epsilon}\cdot\boldsymbol{E})^i & = & J\,\overleftrightarrow{g}^{-1} & \cdot & \overleftrightarrow{\mu} & \cdot & \overleftrightarrow{\epsilon}_{sbh} & \cdot & \overleftrightarrow{\mu}^{-1} & \cdot & \boldsymbol{E}_i \\
m' & & & & \ell_3 & & \ell_2 & & \ell_1 & & m \\
n' & & & & k_3 & & k_2 & & k_1 & & n
\end{array}
$$

therefore

$$
\begin{aligned}
m'' &= m+\ell_1+\frac{1}{2}\ell_2 \qquad & n'' &= n+k_1+\frac{1}{2}k_2 \\
m' &= m+\ell_1+\ell_2+\ell_2 \qquad & n' &= n+k_1+k_2+k_3
\end{aligned}
$$

Destabilization by Energetic Ion

- **Drift kinetic equation**

$$\left[\frac{\partial}{\partial t} + v_\parallel \nabla_\parallel + (\boldsymbol{v}_\mathrm{d} + \boldsymbol{v}_\mathrm{E}) \cdot \boldsymbol{\nabla} + \frac{e_\alpha}{m_\alpha}(v_\parallel E_\parallel + \boldsymbol{v}_\mathrm{d} \cdot \boldsymbol{E})\frac{\partial}{\partial \varepsilon}\right] f_\alpha = 0$$

where

$$\varepsilon = \frac{1}{2} m_\alpha v^2, \qquad \boldsymbol{v}_\mathrm{E} = \frac{\boldsymbol{E} \times \boldsymbol{B}}{B^2}, \qquad \boldsymbol{v}_\mathrm{d} = v_\mathrm{d} \sin\theta \hat{\boldsymbol{r}} + v_\mathrm{d} \cos\theta \hat{\boldsymbol{\theta}}, \qquad v_\mathrm{d} = \frac{m_\alpha}{e_\alpha B R} \cdot \frac{v_\perp^2}{2 + v_\parallel^2}$$

- **Anti-Hermite part of electric susceptibility tensor**

$$\overset{\leftrightarrow}{\chi}_{mm'} = \begin{pmatrix} 1 & -\mathrm{i} & 0 \\ -\mathrm{i} & -1 & 0 \\ 0 & 0 & 0 \end{pmatrix} P_{m-1,m-2}\delta_{m',m-2} + \begin{pmatrix} 0 & 0 & Q_{m-1,m-1} \\ 0 & 0 & -\mathrm{i}\, Q_{m-1,m-1} \\ Q_{m,m-1} & -\mathrm{i}\, Q_{m,m-1} & 0 \end{pmatrix} \delta_{m',m-1}$$

$$+ \begin{pmatrix} (P_{m-1,m} + P_{m+1,m}) & \mathrm{i}\,(P_{m-1,m} - P_{m+1,m}) & 0 \\ -\mathrm{i}\,(P_{m-1,m} - P_{m+1,m}) & (P_{m-1,m} + P_{m+1,m}) & 0 \\ 0 & 0 & R_{m-1,m-1} \end{pmatrix} \delta_{m',m}$$

$$+ \begin{pmatrix} 0 & 0 & Q_{m+1,m+1} \\ 0 & 0 & \mathrm{i}\, Q_{m+1,m+1} \\ Q_{m,m+1} & \mathrm{i}\, Q_{m,m+1} & 0 \end{pmatrix} \delta_{m',m+1} + \begin{pmatrix} 1 & \mathrm{i} & 0 \\ \mathrm{i} & -1 & 0 \\ 0 & 0 & 0 \end{pmatrix} P_{m+1,m+2}\delta_{m',m+2}$$

- **In the case of Maxwellean velocity distributution**

$$
\begin{aligned}
P_{m,m'} &= \mathrm{i}\,\frac{\omega_{\mathrm{p}\alpha}^2}{2\omega^2}\left(1-\frac{\omega_{*\alpha m'}}{\omega}\right)\frac{\rho_\alpha^2}{R^2}\sqrt{\pi}x_m\left(\frac{1}{2}+x_m^2+x_m^4\right)\mathrm{e}^{-x_m^2} \\
Q_{m,m'} &= \mathrm{i}\,\frac{\omega_{\mathrm{p}\alpha}^2}{2\omega^2}\left(1-\frac{\omega_{*\alpha m'}}{\omega}\right)\frac{\rho_\alpha}{R}\sqrt{\pi}2x_m^2\left(\frac{1}{2}+x_m^2\right)\mathrm{e}^{-x_m^2} \\
R_{m,m'} &= \mathrm{i}\,\frac{\omega_{\mathrm{p}\alpha}^2}{2\omega^2}\left(1-\frac{\omega_{*\alpha m'}}{\omega}\right)\sqrt{\pi}4x_m^3\mathrm{e}^{-x_m^2} \\
x_m &= \omega/|k_{\parallel m}|v_{\mathrm{T}\alpha}, \\
\rho_\alpha &= v_{\mathrm{T}\alpha}/\omega_{\mathrm{c}\alpha}, \\
v_{\mathrm{T}\alpha} &= \sqrt{2T_\alpha/m_\alpha}
\end{aligned}
$$

ICRF Waves in Toroidal Helical Plasmas
(Cold Plasma Model)

LHD ($B_0 = 3\,\mathrm{T}$, $R_0 = 3.8\,\mathrm{m}$)

$f = 42\,\mathrm{MHz}$, $n_{\phi 0} = 20$, $n_{e0} = 3 \times 10^{19}\,\mathrm{m}^{-3}$, $n_\mathrm{H}/(n_\mathrm{He} + n_\mathrm{H}) = 0.235$,

$N_\mathrm{rmax} = 100$, $N_{\theta\mathrm{max}} = 16$ ($m = -7 \ldots 7$), $N_{\phi\mathrm{max}} = 4$ ($n = 10, 20, 30$)

Wave electric field (imaginary part of poloidal component)

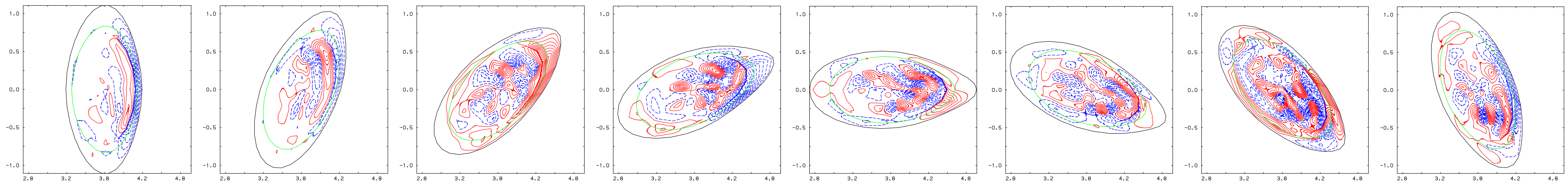

Power deposition profile (minority ion)

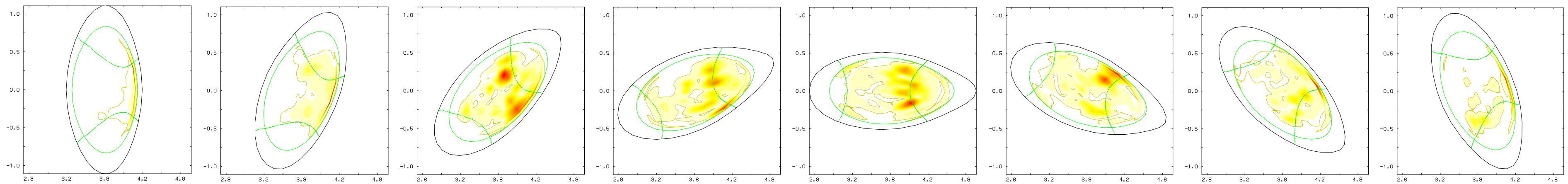

Typical Poloidal Profile

LHD ($B_0 = 3\,\mathrm{T}$, $R_0 = 3.8\,\mathrm{m}$)

$f = 42\,\mathrm{MHz}$, $n_{\phi 0} = 20$, $n_{e0} = 3 \times 10^{19}\,\mathrm{m}^{-3}$, $n_H/(n_{He} + n_H) = 0.235$,

$N_{r\max} = 100$, $N_{\theta\max} = 16$ ($m = -7 \ldots 7$), $N_{\phi\max} = 4$ ($n = 10, 20, 30$)

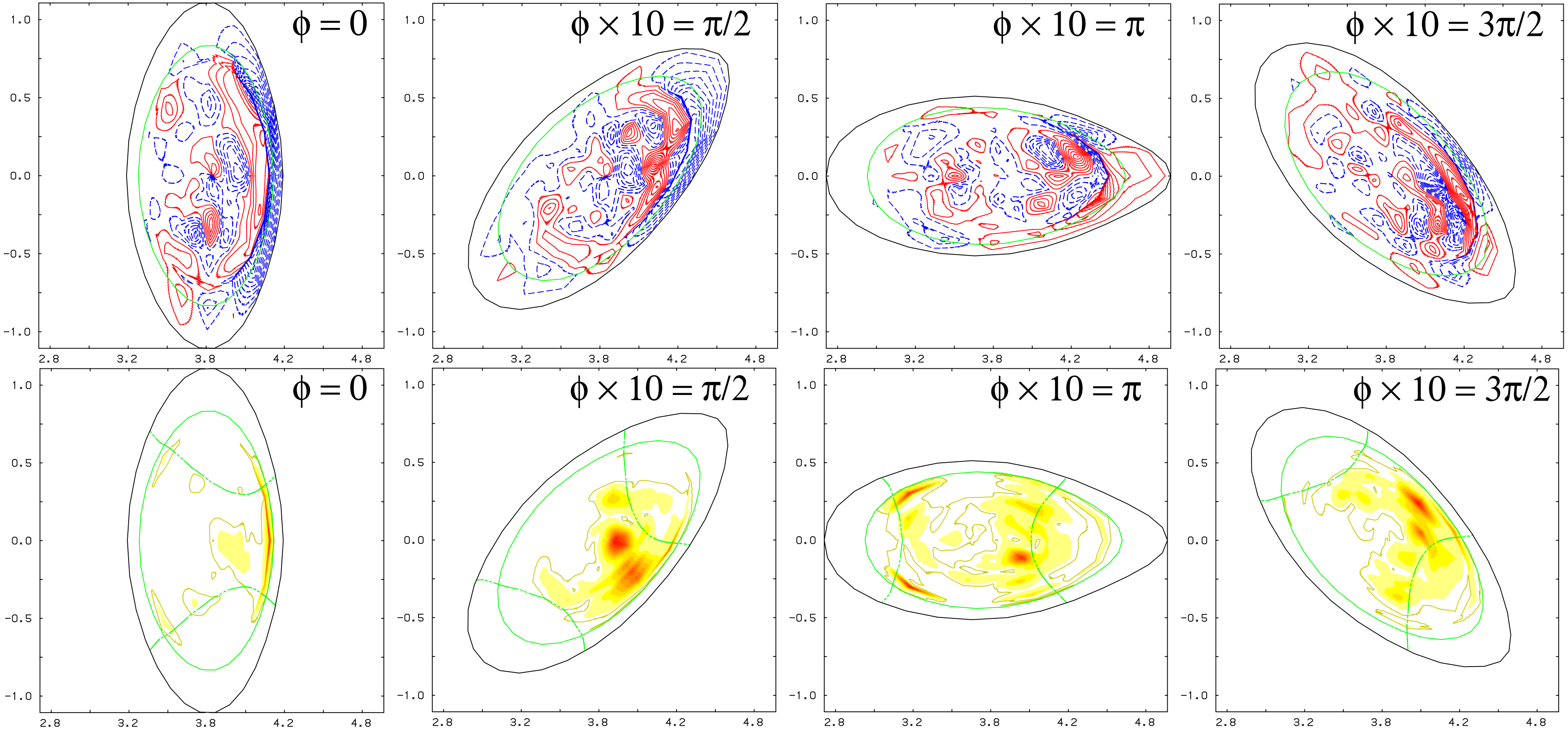

Frequency Dependence

- **Power deposition profile**

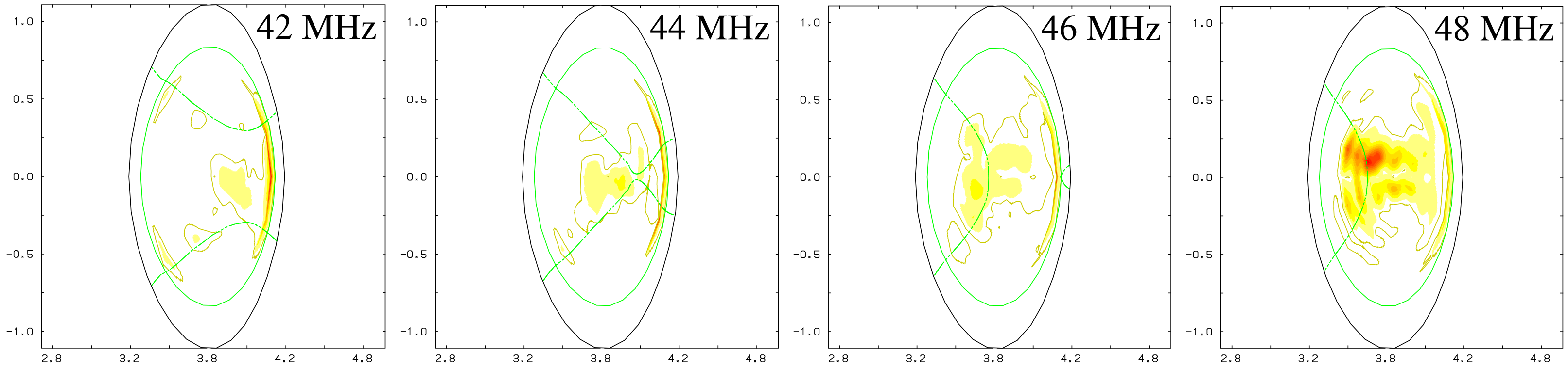

- **Radial deposition profile**

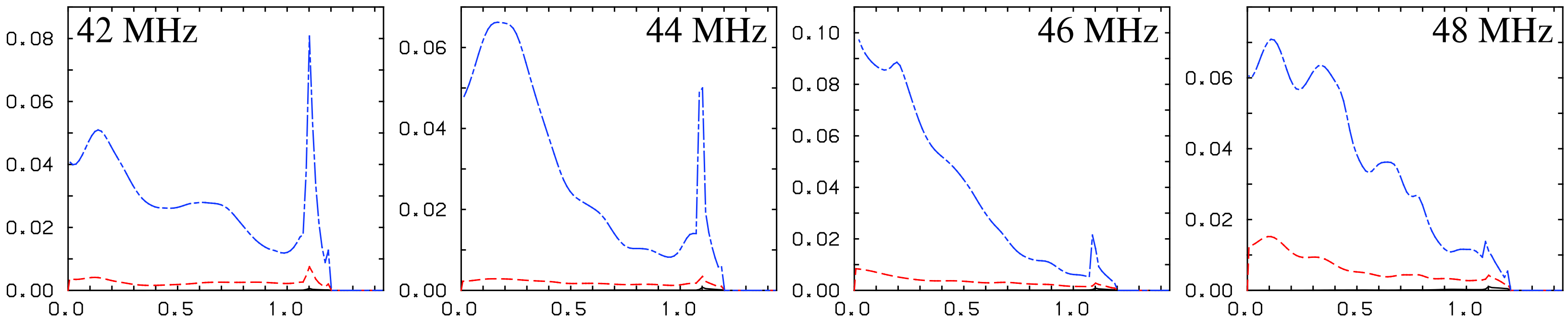

Parameter Dependence

Dependence on n_H Ratio

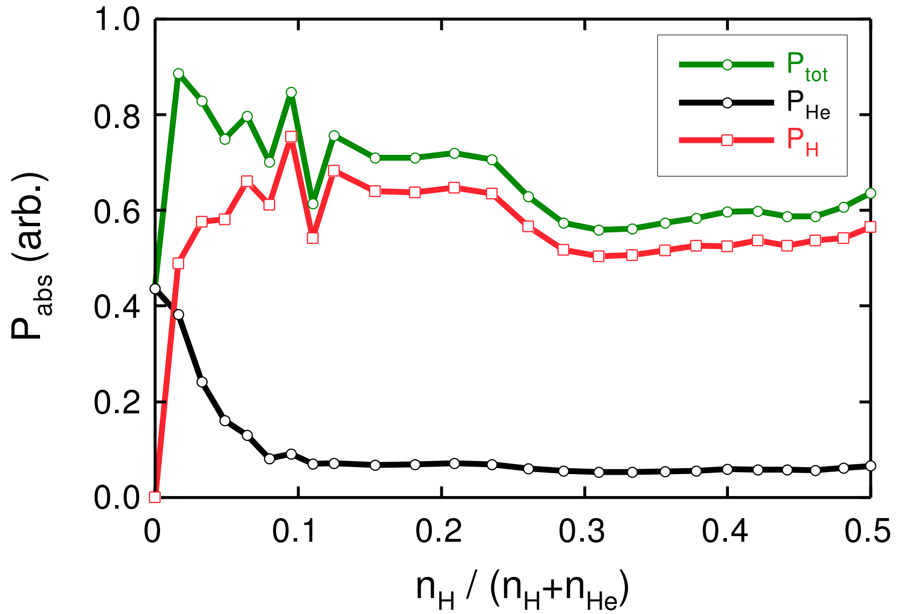

Dependence on $n_{\phi 0}$

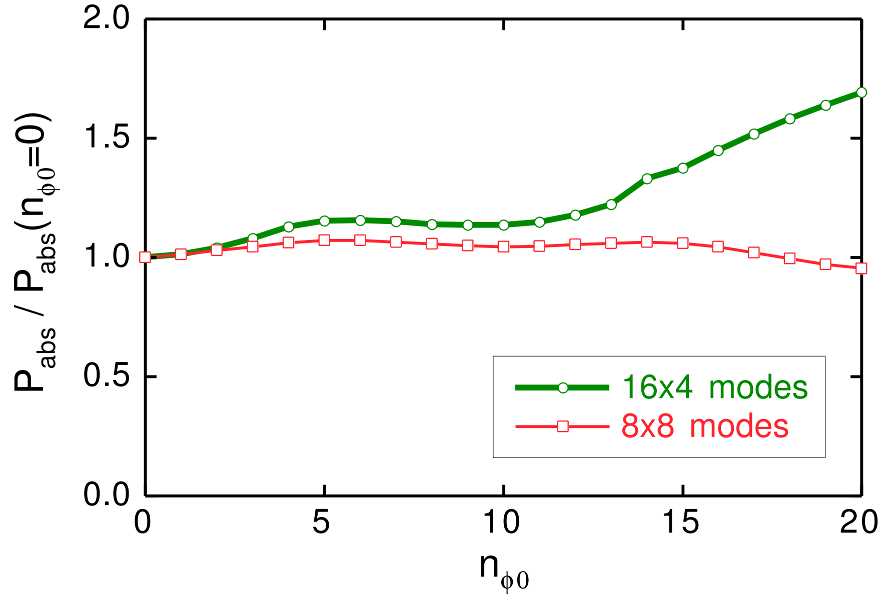

Alfvén Eigenmodes Below Gap requency

Parameters

R	3.5016 m
a	0.9837 m
κ	.2810
δ	0.3098
b/a	1.1
B_0	3.3119 T
I_p	1.6945 MA
$n_e(0)$	0.2356 $10^{20}\mathrm{m}^{-3}$
$n_e(a)$	0.05 $10^{20}\mathrm{m}^{-3}$
$T_e(0)$	4.1 keV
$T_e(a)$	0.8 keV
$T_D(0)$	3.7 keV
$T_D(a)$	0.4 keV

Radial profile of Alfvén resonance frequency

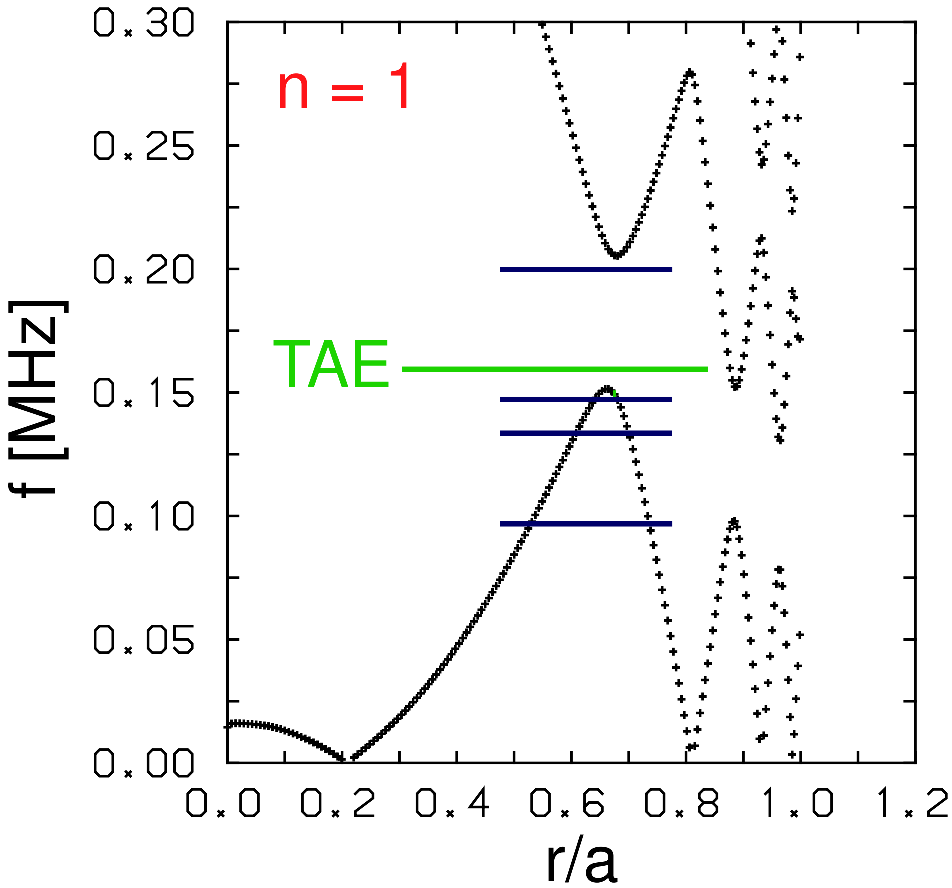

Complex Eigen Frequency of Alfvén Eigenmode

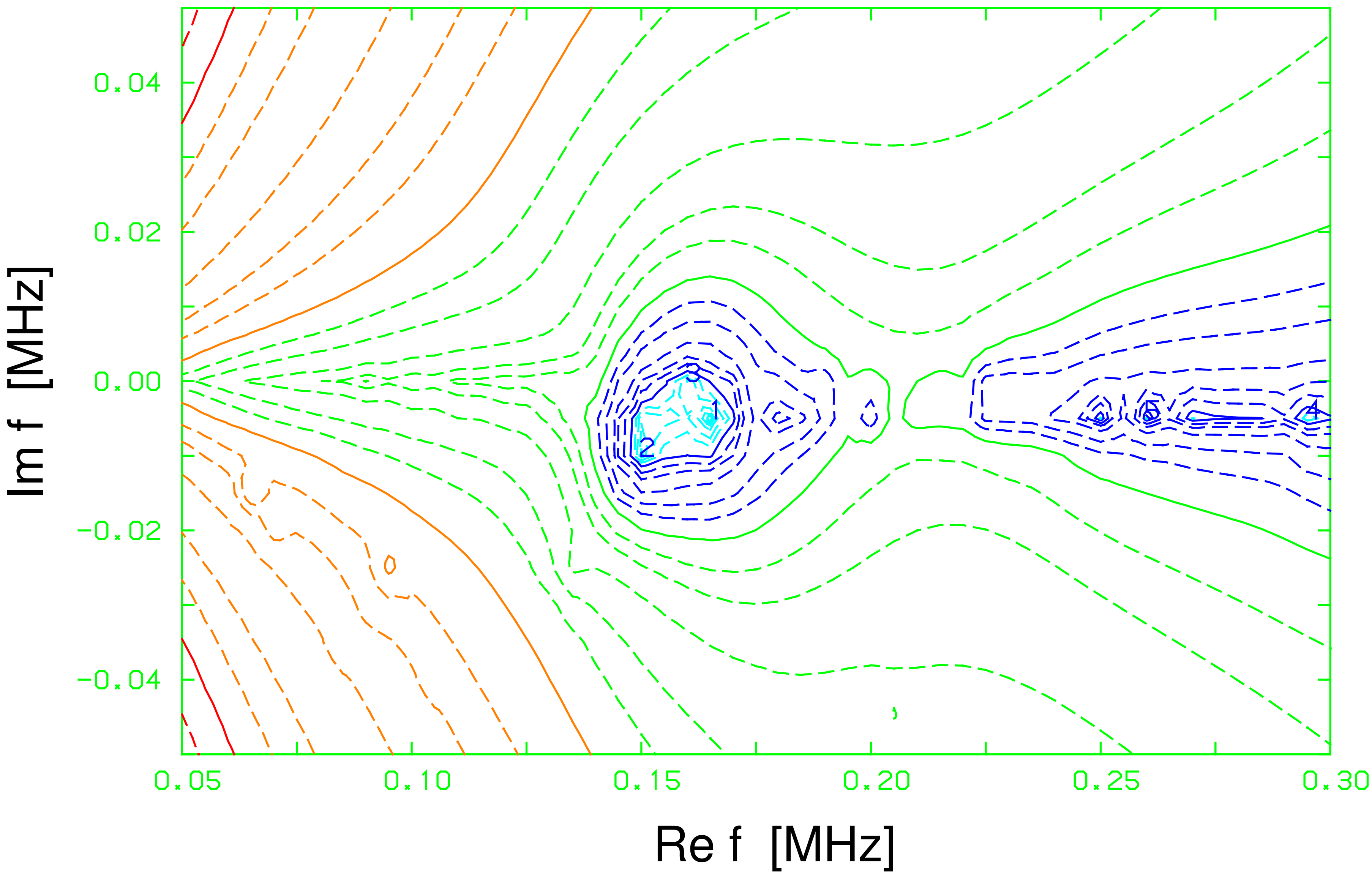

Radial Mode Structure of Alfvén Eigenmode (n = 1)

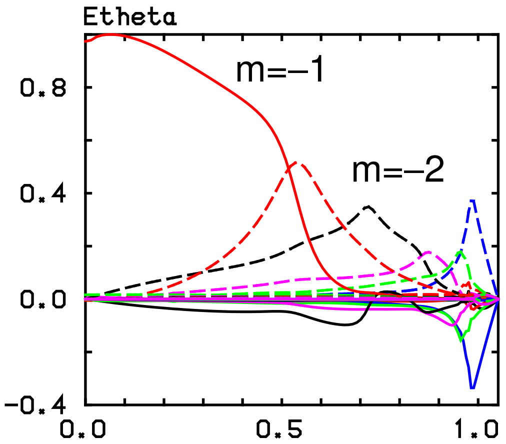

f_r = 97.0 kHz
f_i = −23.6 kHz

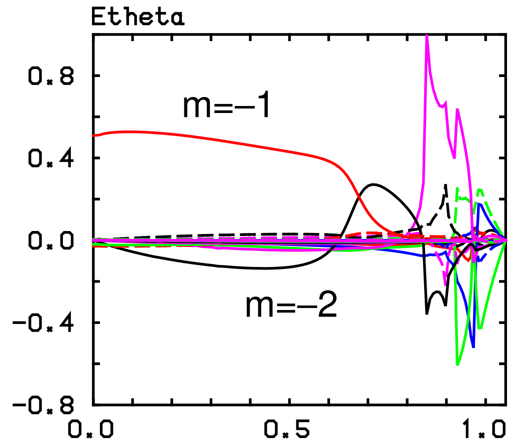

f_r = 199.4 kHz
f_i = −3.37 kHz

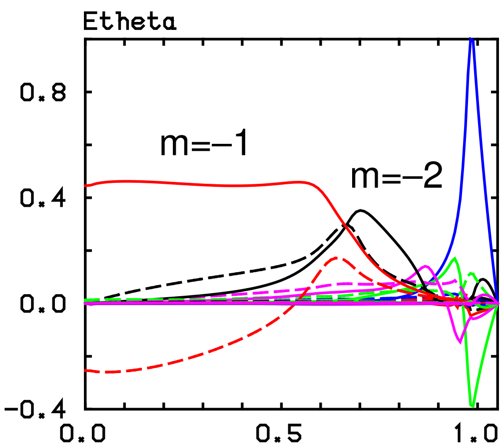

f_r = 136.4 kHz
f_i = −24.1 kHz

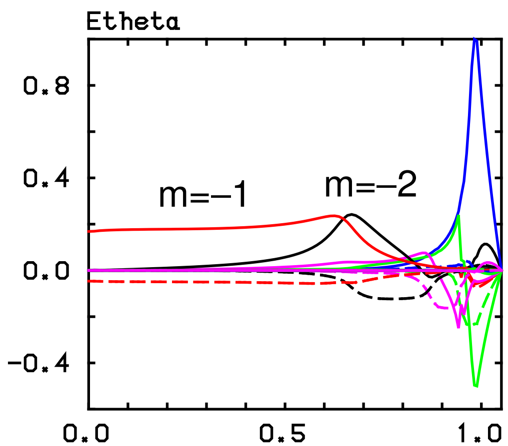

f_r = 149.8 kHz
f_i = −8.12 kHz

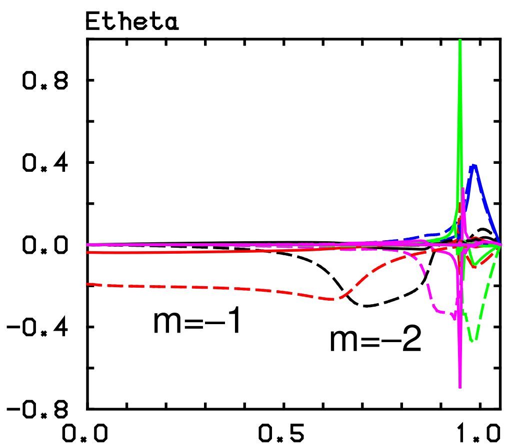

f_r = 164.3 kHz
f_i = −5.08 kHz

Mode Structure with Energetic Particle

- $n_{F0} = 2 \times 10^{17}\,\mathrm{m}^{-3}$, $T_B = 500\,\mathrm{keV}$, $L_{nB} = 0.5\,\mathrm{m}$

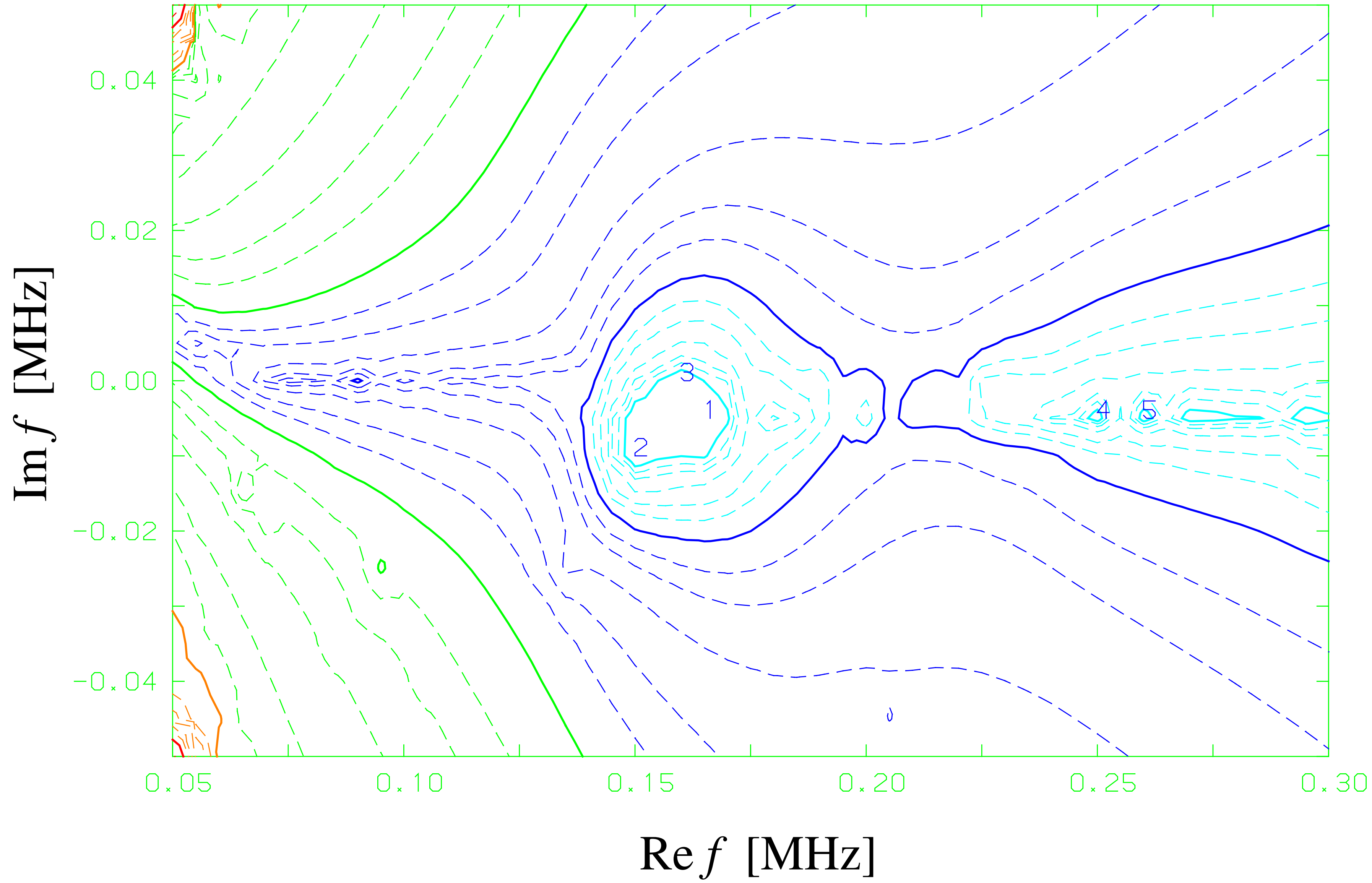

Modes and Eigenfunctions Driven by Energetic Ions

- $n_{F0} = 2 \times 10^{17}\,\mathrm{m}^{-3}$, $T_F = 500\,\mathrm{keV}$, $L_{nF} = 0.5\,\mathrm{m}$, $n = 1$

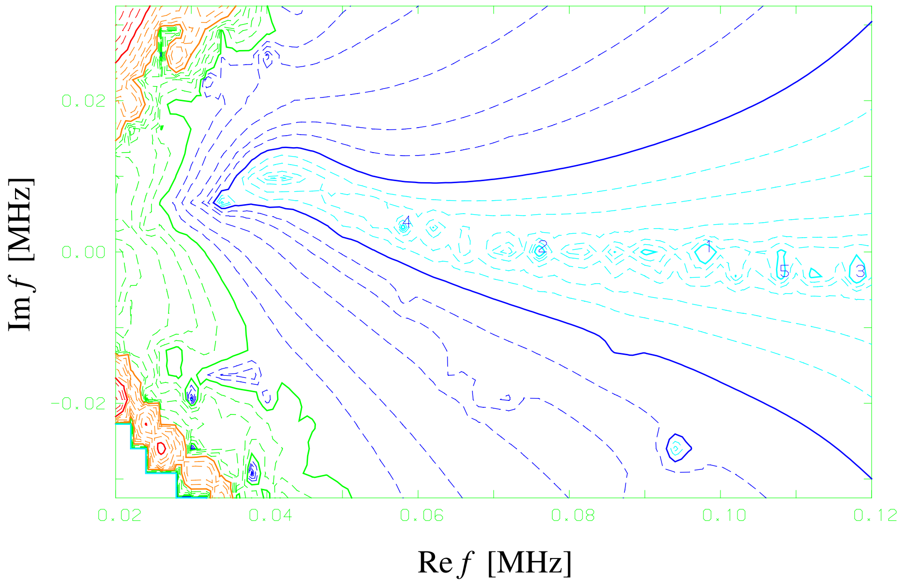

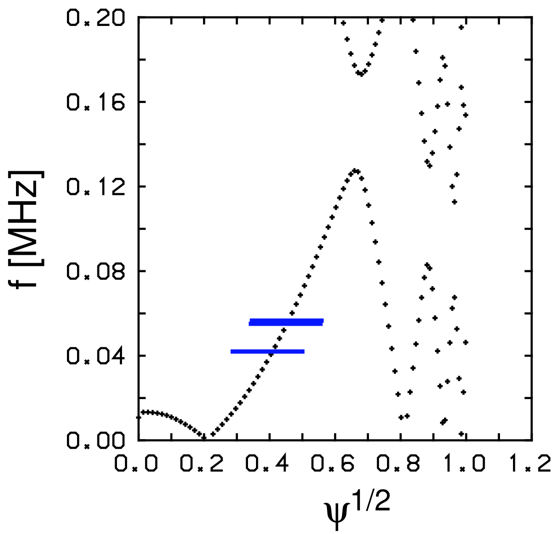

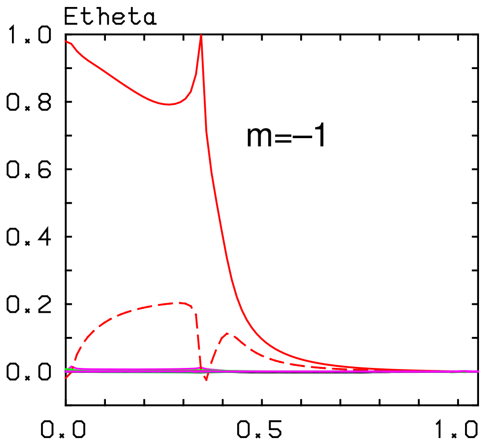

$f_r = 41.8\,\mathrm{kHz}$
$f_i = 8.1\,\mathrm{kHz}$

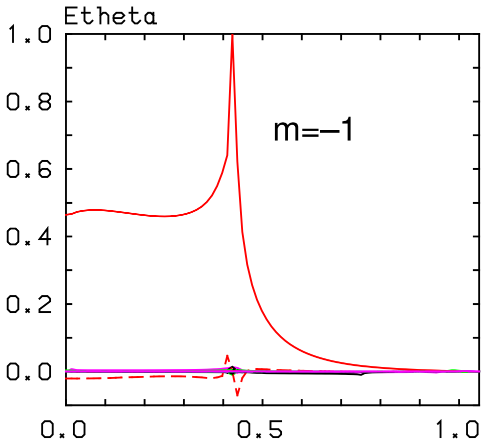

$f_r = 57.7\,\mathrm{kHz}$
$f_i = 3.6\,\mathrm{kHz}$

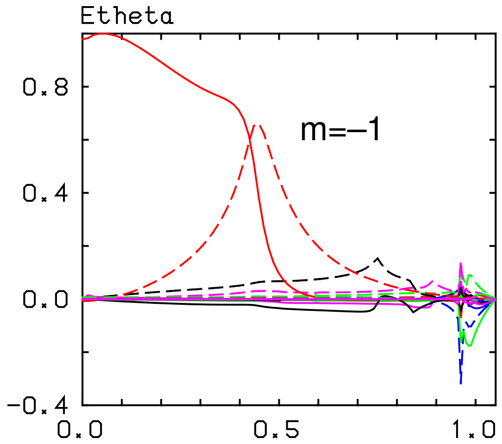

$f_r = 58.0\,\mathrm{kHz}$
$f_i = -6.0\,\mathrm{kHz}$

Parameter Dependence of Mode Structure

$n_{F0} = 0 \times 10^{17}\,\mathrm{m}^{-3}$, $T_B = 0.5\,\mathrm{MeV}$

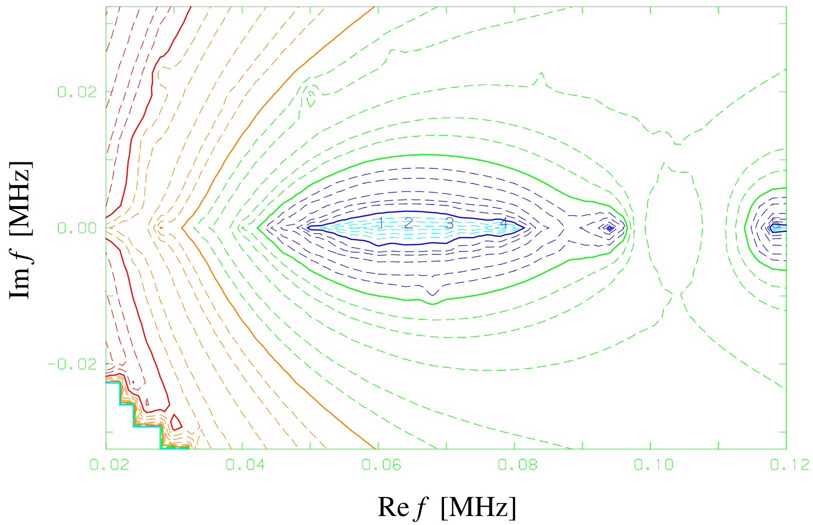

$n_{F0} = 1 \times 10^{17}\,\mathrm{m}^{-3}$, $T_B = 0.5\,\mathrm{MeV}$

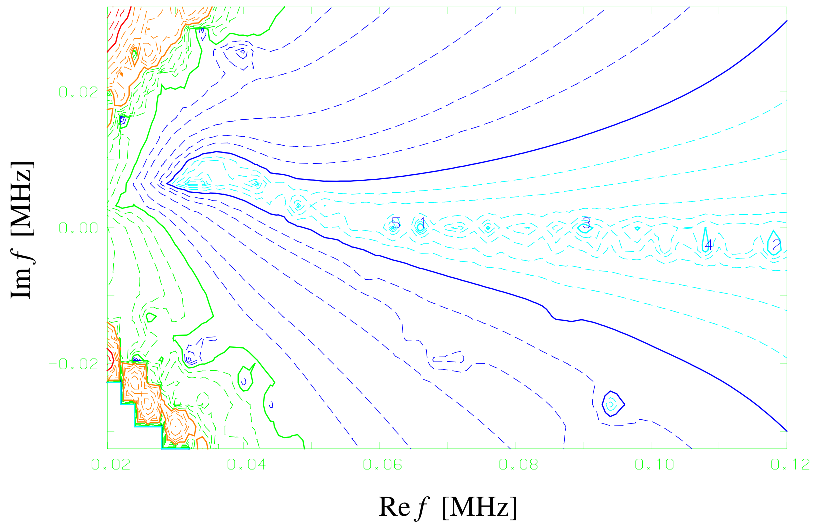

$n_{F0} = 3 \times 10^{17}\,\mathrm{m}^{-3}$, $T_B = 0.5\,\mathrm{MeV}$

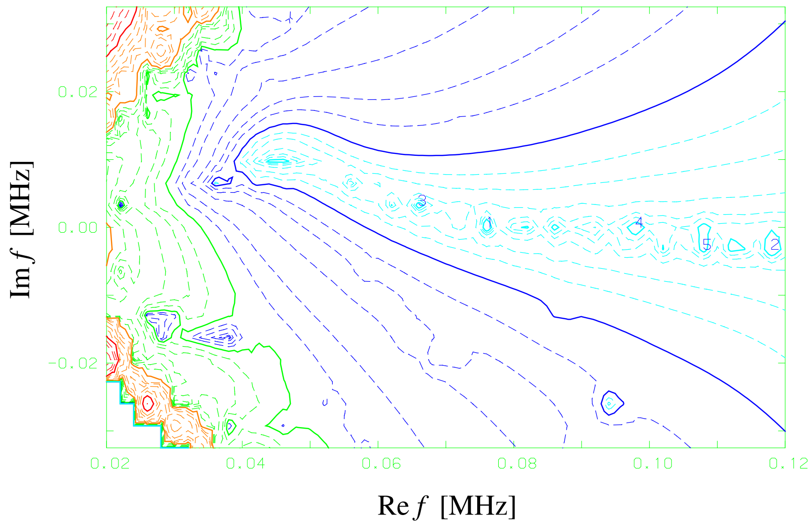

$n_{F0} = 1 \times 10^{17}\,\mathrm{m}^{-3}$, $T_B = 1\,\mathrm{MeV}$

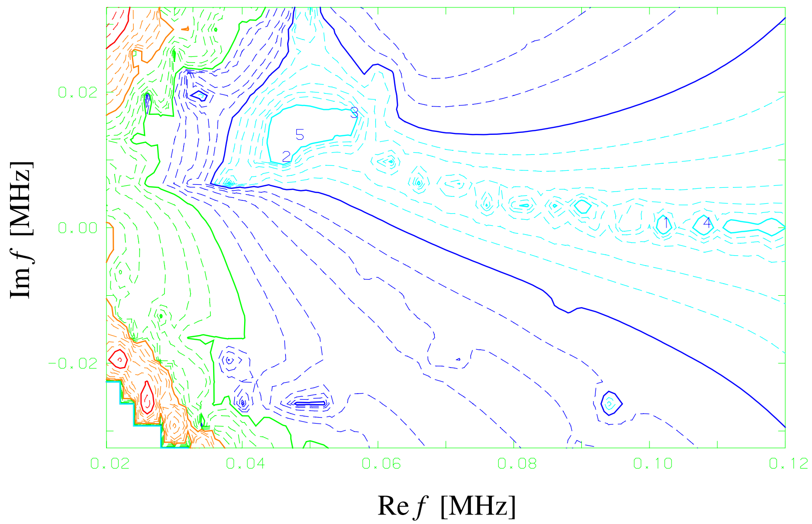

Summary

- We studied ICRF waves in a toroidal helical plasma and Alfvén eigenmodes in tokamak plasmas using the 3D full wave code, TASK/WM.
- Characteristics of ICRF heating in LHD was studies using the cold plasma model. Dependence on the minority ion ratio agrees with experimental observation.
- Kinetic 3D version is now working, but detailed study is not yet completed.
- The mode structure of the EPM/RTAE below the gap frequency was studied. Two types of modes can be destabilized by the energetic ions; strongly damped TAE mode and weakly damped shear Alfvén mode.
- Future work
  - Kinetic analysis of ICRF heating in LHD
  - Systematic analysis of EPM/RTAE destabilized by energetic ions
  - Kinetic Analysis of low-frequency modes including the effect of particle orbit